One-Dimensional Chiral Copper Iodide Chain-Like Structure Cu_4I_4(*R*/*S*-3-quinuclidinol)$_3$ with Near-Unity Photoluminescence Quantum Yield and Efficient Circularly Polarized Luminescence

Jian Chen, Xin Pan, Xuanyu Zhang, Chen Sun, Congcong Chen, Xiaoqin Ji, Rui Chen, and Lingling Mao**

Chiral organic–inorganic hybrid metal halide materials have shown great potential for circularly polarized luminescence (CPL) related applications for their tunable structures and efficient emissions. Here, this work combines the highly emissive Cu_4I_4 cubane cluster with chiral organic ligand *R*/*S*-3-quinuclidinol, to construct a new type of 1D Cu-I chains, namely Cu_4I_4(*R*/*S*-3-quinuclidinol)$_3$, crystallizing in noncentrosymmetric monoclinic $P2_1$ space group. These enantiomorphic hybrids exhibit long-term stability and show bright yellow emission with a photoluminescence quantum yield (PLQY) close to 100%. Due to the successful chirality transfer from the chiral ligands to the inorganic backbone, the enantiomers show intriguing chiroptical properties, such as circular dichroism (CD) and CPL. The CPL dissymmetry factor (g_{lum}) is measured to be ≈4×10^{-3}. Time-resolved photoluminescence (PL) measurements show long averaged decay lifetime up to 10 µs. The structural details within the Cu_4I_4 reveal the chiral nature of these basic building units, which are significantly different than in the achiral case. This discovery provides new structural insights for the design of high performance CPL materials and their applications in light emitting devices.

1. Introduction

Circularly polarized luminescence (CPL) is considered to be a special luminescence phenomenon, which carries a lot of intrinsic information of chiral light-emitting material such as chemical composition and structural symmetry.[1,2] CPL-active materials show great potential applications in circularly polarized light-emitting diodes,[3,4] 3D displays,[5,6] photoelectric devices,[7] memory devices,[8] spintronics,[9,10] optical sensors,[11] and biological probes.[12] The luminescence dissymmetry factor (g_{lum}) is used to quantify the level of CPL and defined as $2 \times (I_{left} - I_{right})/(I_{left} + I_{right})$, where I_{left} and I_{right} are the intensity of the left- and right-handed circularly polarized light, respectively.[13] The theoretical minimum and maximum value of $|g_{lum}|$ is 0 and 2, corresponding to nonpolarized and completely left/right-circularly polarized emissions, respectively.[14] Generally, typical CPL-active materials consist of two major moieties: chiral nonluminescent and achiral luminescent building blocks, which self-assemble into chiral structures. The chirality can be transferred from the chiral centers to the achiral components, leading to overall CPL emission.[1] In addition, the chiral materials can exhibit other intriguing properties, such as ferroelectricity, piezoelectricity, and pyroelectricity.[15]

In an attempt to obtain high-performance CPL materials, great efforts have been made based on organic–inorganic hybrid metal halides combining chiral organic molecules.[16,17] For example, enantiomorphic chiral hybrids *R*/*S*-$C_6H_{15}Cl_2NO{\bullet}SbCl_5$, exhibit intense emission with a photoluminescence quantum yield (PLQY) of 71.2% and CPL activity with a g_{lum} of 2.5×10^{-4}.[18] We reported 1D chain-like hybrid manganese bromides, (*R*/*S*-3-quinuclidinol)$MnBr_3$, having a high g_{lum} of 2.3×10^{-2} and a PLQY of 50.2%.[19] 0D hybrid lead-tin bromides, (*RR*/*SS*-$C_6N_2H_{16})_2Pb_{0.968}Sn_{0.032}Br_6{\bullet}2H_2O$, was reported with a g_{lum} of 3.0×10^{-3} and a remarkable PLQY of 100%.[20] However, there are still few reported cases of highly efficient CPL-active hybrids, where quite a lot of them suffer from a low PLQY.[21,22] To consider technical applications, it is highly important to design and construct ideal hybrid metal halides with efficient left or right CPL and high PLQY.

Among the hybrid metal halides, hybrid copper halides have particularly attracted tremendous attentions, for they possess highly diverse structures,[23] magnetic properties,[24,25] and efficient luminescence.[26–31] The combination of the inorganic copper(I) iodides with organic ligands/cations generates

J. Chen, X. Pan, C. Sun, C. Chen, X. Ji, L. Mao
Department of Chemistry
Southern University of Science and Technology
Shenzhen, Guangdong 518055, P. R. China
E-mail: chenj6@sustech.edu.cn; maoll@sustech.edu.cn
X. Zhang, R. Chen
Department of Electrical and Electronic Engineering
Southern University of Science and Technology
Shenzhen, Guangdong 518055, P. R. China
The ORCID identification number(s) for the author(s) of this article can be found under https://doi.org/10.1002/smll.202300938.

DOI: 10.1002/smll.202300938

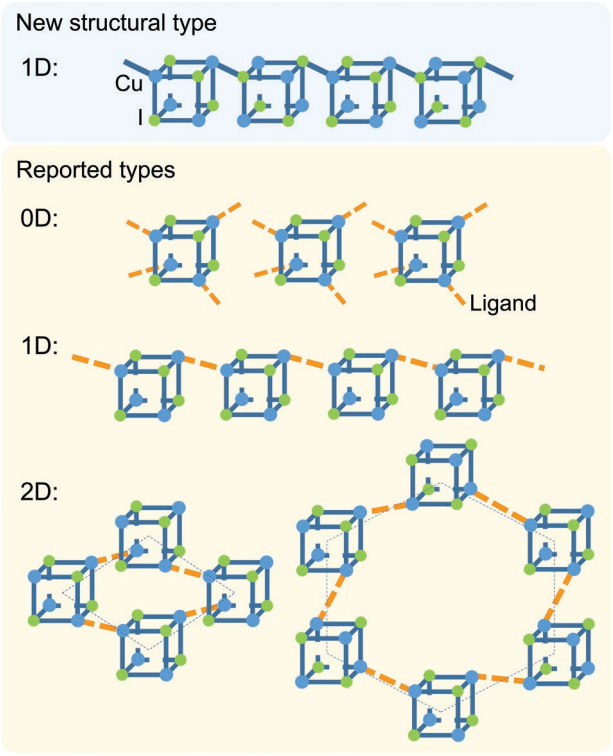

Scheme 1. New structural type in this work and reported types of hybrid copper(I) iodides built by Cu_4I_4 cubane tetramers. Cu and I atoms are represented by blue and green spheres, respectively. Orange dotted lines represent links through organic ligands. Navy blue lines represent the coordination bonds between Cu and I.

a large variety of hybrid structures. Thousands of hybrid copper(I) iodides have been reported in the Cambridge Crystallographic Data Centre (CCDC) database. An appropriate selection of organic components allows the target materials showing intriguing optical phenomena, such as high brightness,[32,33] CPL emission,[34–36] second harmonic generation,[36,37] thermochromism,[38] and mechanochromism.[39,40]

The most extensively studied structural type is the charge-neutral inorganic module (Cu_nI_n) coordinated with N-, P-, S-, Sb-, or Se-donor ligands (*L*), forming 0D discrete cluster, 1D chain, 2D network, and 3D framework.[28,29] In 0D discrete structures, the Cu_nI_n nanocluster takes various forms, including Cu_2I_2 rhomboid dimer,[30,32] Cu_3I_3 trimer,[41] Cu_4I_4 staircase tetramer,[42] Cu_4I_4 cubane tetramer,[30,34] Cu_6I_6 eared cubane hexamer,[43] Cu_6I_6 staircase hexamer,[44] Cu_7I_7 pinwheel heptamer,[45] Cu_7I_7 heptamer,[46] Cu_8I_8 staircase octamer,[47] and Cu_8I_8 double-cubane octamer.[48] In Cu_4I_4 cubane tetramer, the monovalent copper ions typically adopt tetrahedral coordination geometry.[26] This means each [Cu_4I_4] building block offers four unsaturated Cu(I)-binding sites, which could be coordinated with organic ligands to construct the higher dimensional extended structures (**Scheme 1**).[28,29,49,50] The Cu_4I_4 cubane tetramers based hybrid compounds usually exhibit bright emission with high PLQYs, comparing with other Cu_nI_n nanoclusters.[28,29,51–53] The strong Cu–Cu interactions as a result of short Cu–Cu interatomic distances in these Cu_4I_4 cubane tetramers, generally lead to cluster-centered (CC) luminescence.

In this work, we utilize the highly emissive nature of Cu_4I_4 cubane tetramer combining with chiral ligands to develop novel high-performance CPL materials. A pair of chiral ligands, *R*/*S*-3-quinuclidinol, which has large molecular size, high steric hindrance, and appropriate N-donor, was employed here to form a stable and rigid 1D chain-like structure.[19] An enantiomeric pair of Cu_4I_4 cubane tetramer-based 1D copper-iodine chains, formulated as Cu_4I_4(*R*/*S*-3-quinuclidinol)$_3$ (abbreviated as *R*/*S*-**1**), is first reported here as a new structural type (Scheme 1). *R*-**1** and *S*-**1** possess distinct chiral characteristics and a near-unity PLQY (≈100%) at room temperature. The g_{lum} values of powdered samples of *R*-**1** and *S*-**1** are 4.3×10^{-3} and -4.1×10^{-3}, respectively. We have found the *R*/*S*-**1** Cu_4I_4 unit undergoes significant structural distortion with a helical twist angle of 11° and deviation in the Cu-I bond length, which is significantly different from the achiral 0D compound. This work provides new design guidelines and structural insights for next-generation high performance hybrid materials for chiroptical applications.

2. Results and Discussion

An amount of 2 mL saturated KI aqueous solution containing 0.5 mmol CuI (bottom layer), 1 mL mixed solution of ethanol and water (buffer layer), and 2 mL ethanol containing 0.5 mmol *R*/*S*-3-quinuclidinol (top layer) was placed in a narrow-diameter glass tube in order (see **Figure 1**). Shiny, colorless, plate-like crystals *R*/*S*-**1** were obtained within 1 week through a slow diffusion between the top layer and bottom layer at room temperature. For the synthesis part, temperature is one key factor of influencing the crystal growth and its packing mode. Generally, low temperature reduces diffusion rate and leads to the growth of high quality crystals. Single-crystal X-ray diffraction (SC-XRD) analysis at 298 K reveals that *R*/*S*-**1** crystallize in noncentrosymmetric, monoclinic $P2_1$ space group, where the detailed crystallographic data is shown in Table S1 (Supporting Information). The trilobed propeller-like asymmetric unit contains one Cu_4I_4 cubane tetramer coordinated with three N atoms from *R*/*S*-3-quinuclidinol ligands, forming a 1D chain-like structure in the direction of *a*-axis (**Figure 2**). Each [Cu_4I_4] building block is connected to its neighboring cubane through a Cu-I bond ($d_{Cu\text{-}I}$ = 2.69 Å) (Scheme 1 and Figure 2). The Cu–Cu distances are shorter than or close to the sum of the van der Waals radii of copper(I) (2.80 Å),[54] indicating that intramolecular cuprophilic bonding interactions are present in *R*/*S*-**1** (Table S2, Supporting Information).[55] It is worth noting that this new 1D type structure is reported here for the first time, where usually in Cu(I) iodides the extended structures are linked via organic ligands. The powdered samples of *R*/*S*-**1** used in the following characterizations were macroscopically examined by powder X-ray diffraction (PXRD) and then compared with the simulated patterns determined by SC-XRD analysis (Figure 1 and Figure S1, Supporting Information). These 1D materials exhibit good stability against moisture and oxidation, where the PXRD of *R*-**1** sample stored in atmosphere for 1000 h remains unchanged (Figure S2, Supporting Information). Interestingly, using the racemic ligand, *Rac*-3-quinuclidinol, leads to the formation of a reported 0D structure Cu_4I_4(*Rac*-3-quinuclidinol)$_4$ (*Rac*-**1**) (Figure 1).[56] *Rac*-**1** crystallizes in centrosymmetric,

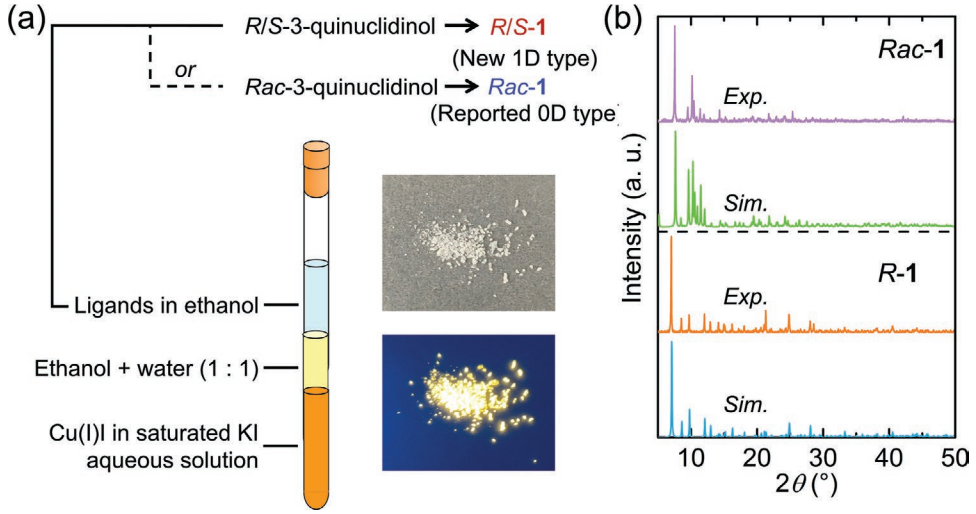

Figure 1. a) Synthesis of 0D Cu_4I_4(*Rac*-3-quinuclidinol)$_4$ (*Rac*-**1**) and 1D Cu_4I_4(*R*/*S*-3-quinuclidinol)$_3$ (*R*/*S*-**1**). Insert: pictures of polycrystalline *R*-**1** under daylight (upper) and ultraviolet (UV) flashlight (down). b) Experimental and simulated X-ray powder diffractograms for *Rac*/*R*-**1**.

monoclinic *C*2/*c* space group. The discrete asymmetric unit of *Rac*-**1** contains one Cu_4I_4 cubane coordinated with four *Rac*-3-quinuclidinol ligands (Figure S3, Supporting Information).

As shown in **Figure 3**a and Figure S4a (Supporting Information), the absorption spectra of the polycrystalline *R*-**1** and *S*-**1** exhibit a broad shoulder at 400 nm, and three weak bands at 315, 263, and 204 nm. The absorption peaks at 263 and 204 nm are identical to pure *R*/*S*-3-quinuclidinol (Figure S4b, Supporting Information). This confirms that these two peaks are assigned to absorption by the organic components. The peaks at 400 and 315 nm are assigned to the inorganic components, which are consistent with the reported chiral hybrid copper(I) iodides built by Cu_4I_4 cubane tetramer.[34] To confirm the successful transfer of chirality of *R*-**1** and *S*-**1**, the circular dichroism

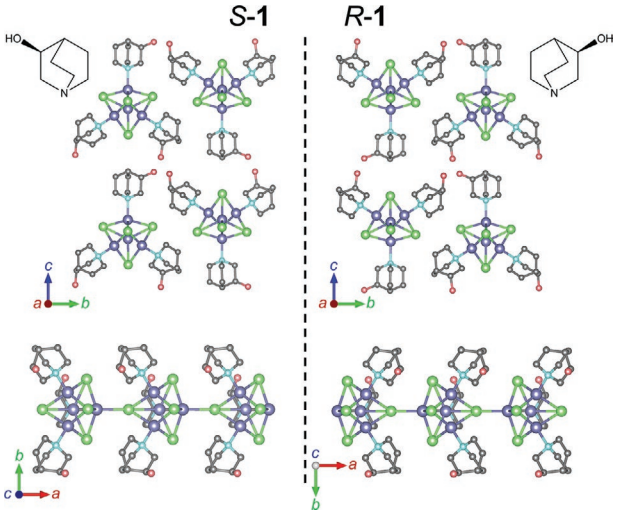

Figure 2. Enantiomorphic crystal structures along the *a*-axis (upper) and the view of 1D chains in the direction of *a*-axis (down) of *S*-**1** (left) and *R*-**1** (right). Cu, I, C, N, and O atoms are colored in violet, green, grey, cyan, and red, respectively. Hydrogen atoms are omitted for clarity. Black dotted line represents mirror plane. Inset: chemical structural formula of *R*/*S*-3-quinuclidinol.

(CD) measurements, which show the differential absorption ability of a chiral material to left-handed and right-handed CP light, were conducted on the polycrystalline samples at room temperature. Mirrored CD signals appear at approximately 400 nm, which is in agreement with the main absorption peak (Figure 3b). The Cotton effect shifts absorption spectra for left-handed CP versus right-handed CP light, resulting in the characteristic dispersive feature in CD spectroscopy.[16] These CD responses stem from the Cotton effect of absorption bands of Cu_4I_4 cubane tetramer, influenced by the coordinated chiral *R*/*S*-3-quinuclidinol. This result indicates that the chirality is efficiently transferred to the inorganic components from the coordinated chiral organic ligands. An absorption anisotropy factor (g_{CD}) is employed quantify the intrinsic CD, and calculated using the following equation: $g_{CD} = (A_{left} - A_{right})$/absorbance = CD [mdeg]/(32 980 × absorbance).[57] A_{left} and A_{right} are the absorbances of left-handed and righthanded CP lights. The g_{CD} values of *R*-**1** and *S*-**1**, calculated at the absorption peak at 400 nm, are 2.6×10^{-3} and -1.6×10^{-3}, respectively (**Table 1** and Figure S5, Supporting Information). The g_{CD}s are on the order of 10^{-3}, which are in accordance with the magnitude of previously reported chiral hybrid metal halides measured on their polycrystalline form.[19,58]

The optical bandgaps were determined by diffuse reflectance spectroscopy measurements on polycrystalline samples (Figure S6, Supporting Information). Extrapolation of the absorbing edge to the linear part gave the bandgap values of 2.86 and 2.90 eV for *R*-**1** and *S*-**1**, respectively, which correspond with transparent and colorless crystals (Table 1 and **Figure 4**a). These bandgaps are comparable with other reported Cu_4I_4 cubane-based hybrid copper(I) iodides.[28]

To further characterize the optical properties of these materials, we have conducted steady-state and time-resolved photoluminescence (PL) measurements. The optical properties of *R*/*S*-**1** are summarized in Table 1. *R*-**1** and *S*-**1** exhibit highly emissive yellow light emission under ultraviolet (UV) lamp irradiation (Figure 4a and Figure S7, Supporting Information). Both compounds have almost identical PL emission spectra

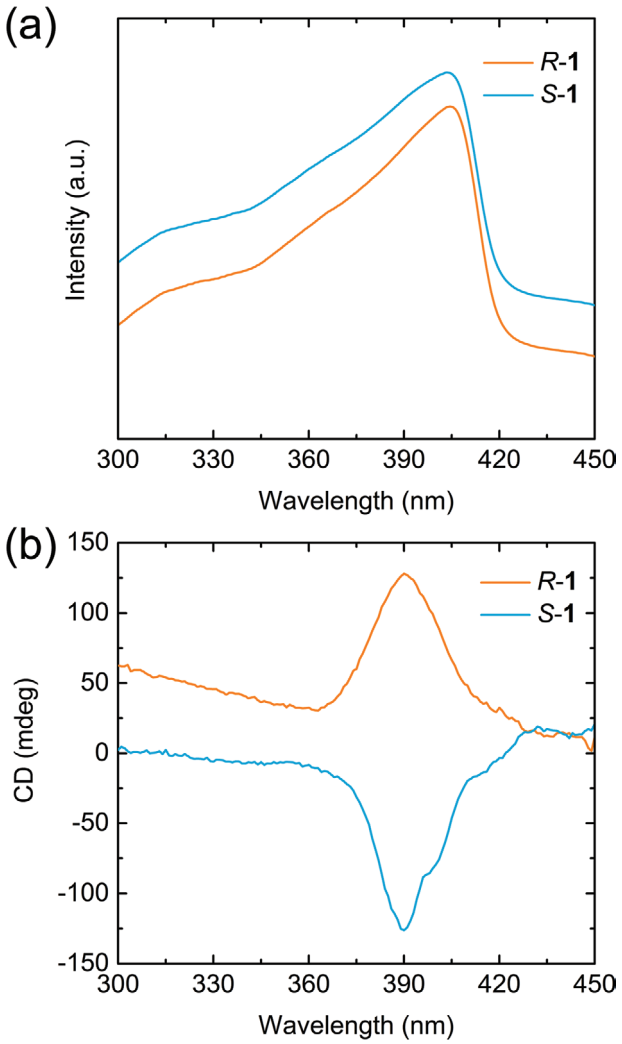

Figure 3. a) Circular dichroism (CD) spectra of polycrystalline *R*/*S*-**1**, matching well with the absorbance spectra peak. b) Absorbance spectra of polycrystalline *R*/*S*-**1**.

(Figure 4b) with a peak centered at 575 nm. With the Gaussian fitting, the full width at half-maximum (fwhm) of these emission peaks are 115 nm. The excitation spectra of these two compounds are also the same, and the highest PL intensity should be excited with λ_{ex} of 375 nm. The Stokes shift is determined to be 200 nm, which is similar to those of many previously reported Cu_4I_4 cubane tetramer-based halides.[28] The large Stokes shift is useful for avoiding the self-absorption issue. The PL mechanism of *R*/*S*-**1** are similar to those of reported [Cu_4I_4] cluster complexes.[59] The short Cu–Cu distances inside the Cu_4I_4 clusters, such as 2.534(1) Å for *R*-**1** and 2.5300(9) Å for *S*-**1**, support the existence of a "metal cluster centered" excited state. And the PL emission can be attributed to a triplet "cluster centered" (^{3}CC*) excited state, which involves iodide-to-metal charge transfer (^{3}XMCT*) and "metal cluster centered" (^{3}MCC*, $d^{10}Cu \rightarrow d^9s^1Cu$) characters.[60] Through double-exponentially fitting the time-resolved PL decay spectra, we obtained the lifetimes of 10.76 and 10.42 µs for *R*-**1** and *S*-**1**, respectively (Figure 4c).

Table 1. Summary of the optical properties of *R*/*S*-**1**.

Compounds	*R*-**1**	*S*-**1**
λ_{ex} [nm]	375	
λ_{em} [nm]	575	
fwhm [nm]	115	
Stokes shift [nm]	200	
PLQY [%]	99.9	99.8
Bandgap [eV]	2.86	2.90
Lifetime [µs]	10.76	10.42
g_{CD} [$\times 10^{-3}$]	2.6	−1.6
g_{lum} [$\times 10^{-3}$]	4.3	−4.1

The PLQYs of the polycrystalline samples are measured to be near-unity, 99.9% for *R*-**1** and 99.8% for *S*-**1**, with 365 nm excitation at room temperature (Table 1). As far as we know, there are only a few reported hybrid copper(I) iodides showing PLQY exceeding 99%. The 0D isolated structure *Rac*-**1** with low rigidity, was reported to has a PLQY of 30%,[56] which is quite lower than *R*/*S*-**1**. The high PLQYs of *R*/*S*-**1** are likely due to the suppression of nonradiative decay in rigid structures.[28,29,51–53,61] The near-unity PLQY was also observed in another reported 1D chain-like hybrid copper(I) iodide cluster, (4-dimethylamino-1-ethylpyridinium)$_2Cu_4I_6$, which possesses rigid environment inside skeleton.[61] The hydrogen bonding interactions are formed between oxhydryls in organic ligands from adjacent [Cu_4I_4(*R*/*S*-3-quinuclidinol)$_3$]$_\infty$ chains (Figure S8, Supporting Information). The O···O distances in three H-bonds in *R*-**1** are 2.750 Å, 2.818 Å, and 2.844 Å, respectively. These high sterically hindered *R*/*S*-3-quinuclidinol ligands with strong H-bonding interactions, build a rigid network by self-assembly with [Cu_4I_4] building blocks. The rigid and stable trilobed propeller-like chain structures could restrain the molecular vibration and rotation, preventing energy transfer.

Based on the chiral structure and ultrabright yellow emission, strong CPL signals are realized in these new materials. *R*-**1** and *S*-**1** exhibit mirror-image profiles in their CPL emission spectra, measured on single crystal and powdered form (Figure S9a, Supporting Information, and **Figure 5**a). *R*-**1** and *S*-**1** show the left-handed signal and right-handed CPL signal, respectively. CPL spectra are consistent with the regular PL spectra regarding the emission width and the peak position (Figure 3b). The g_{lum} values of single crystals of *R*-**1** and *S*-**1** at their maximum emission wavelength are $+1.48 \times 10^{-1}$ and -1.42×10^{-1}, respectively (Figure S9b, Supporting Information). In addition to our case, the high g_{lum} values on the order of 10^{-1} were also observed in single crystals of other compounds.[19,21,62] Such high g_{lum}s were induced by the effect of linear polarized light (LPL) and birefringence or a circular Bragg phenomenon, which cannot be ignored in the CPL measurements using single crystals with large anisotropy.[62,63] LPL effect could magnify the detected CPL intensity. Because of this, a change of orientation, size, or shape of single crystals will lead to the variation in direction and intensity of detected CPL signals.

To avoid the anisotropy of single crystals, we ground the samples of *R*/*S*-**1** more than 15 min, and obtained their powdered form. The g_{lum} values of powdered *R*-**1** and *S*-**1**

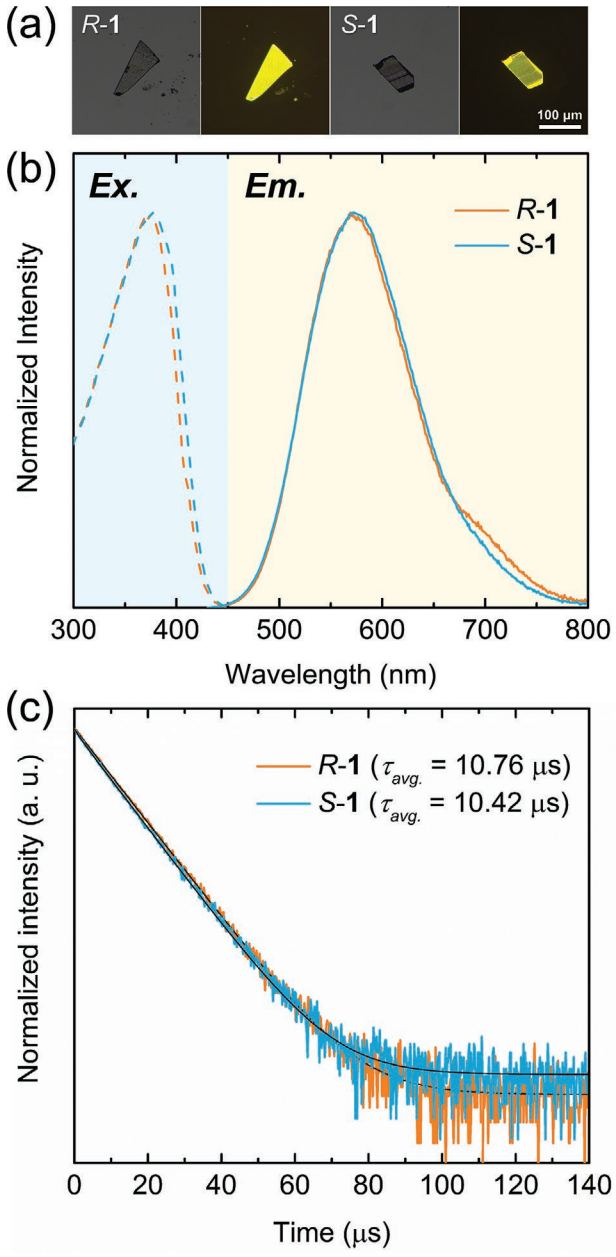

Figure 4. a) Optical microscopic pictures of plate-like crystals of *R*/*S*-**1** under daylight and ultraviolet (UV) flashlight (330–385 nm). b) Normalized excitation and emission spectra. c) Time-resolved photoluminescence (PL) decay spectra.

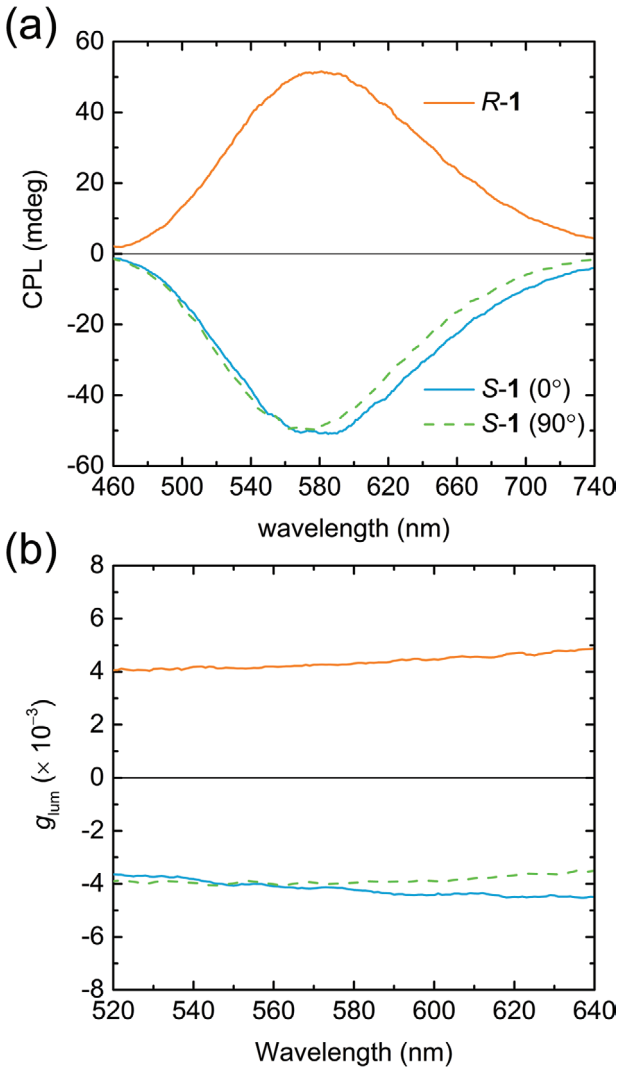

Figure 5. C. ircularly polarized luminescence (CPL) emission spectra (a), and g_{lum} versus wavelength curves (b) of powdered *R*/*S*-**1**. The curves of *R*-**1** and *S*-**1** are shown in orange and blue, respectively. The green dotted lines represent the curves of sample after 90° clockwise rotation.

calculated from the mirror-image CPL spectra at maximum emission wavelength are $+4.3 \times 10^{-3}$ and -4.1×10^{-3}, respectively, which are at the same level as those of other reported CPL-active chiral hybrid copper(I) iodides (Figure 5a).[34–36] The CPL was also measured on the powdered *S*-**1** after 90° clockwise rotation, and gave a g_{lum} of -4.0×10^{-3} (Figure 5b). The CPL intensity and g_{lum} value obtained at rotation angles of 90° are almost identical to the data at 0°. It can be seen that there is no significant change in spectral shape with rotation angle, indicating they are anisotropy artifact free. The CPL signals stem from intrinsic chirality of inorganic parts, induced by the direct connection of the chiral ligands to the inorganic cubanes through coordination bonds.[19] There are six different Cu–Cu distances between the two neighboring Cu atoms in the distorted tetrahedral Cu_4^{4+} unit (Table S2 and Figure S10, Supporting Information). Therefore, these four Cu atoms can be viewed as a new chiral tetrahedral unit. In addition, the CPL spectra are determined by the electric and magnetic transition dipoles, which are influenced by the degree of helical twist in Cu_4I_4 cubane.[64] In our case, the helical twist angle (θ) of *R*/*S*-**1** are approximately 11.6°, which is higher than the value of 5° in previously reported chiral analogues and different from *Rac*-**1** (nearly 0°) (**Figure 6**).[34] In addition to the θ difference, the Cu-I bond length also varies to a larger degree in *R*/*S*-**1** (Figure 6). These observations further validate the chiral nature of the as-synthesized 1D materials, in sharp contrast to the *Rac*-**1** structure. Both of the skeleton and chiral ligands are critical for design and construction of

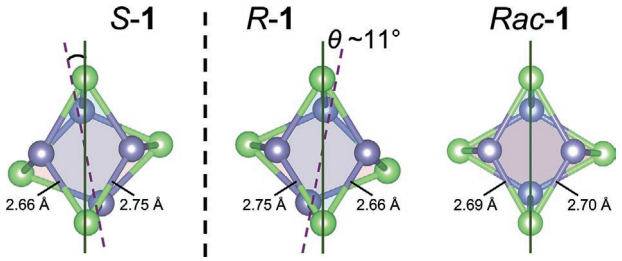

Figure 6. Diagrammatic sketch of helical twist angles (θ) and Cu-I bond lengths in Cu_4I_4 cubane in *R*/*S*-**1** and *Rac*-**1**.

high performance CPL materials. On one hand, Cu_4I_4 cubane tetramer possesses highly emissive nature. On the other hand, the chiral *R*/*S*-3-quinuclidinol ligands, which show large molecular size and high steric hindrance, are helpful to stabilize the structures. The inorganic part achieves "intrinsic" chirality for its helical twist in Cu_4I_4 cubane, induced by the direct connection of chiral ligands, leading to new chiroptical properties. This combination of skeleton together with *R*/*S*-quinuclidinol generates highly efficient CPL materials.

3. Conclusion

In conclusion, we report here a novel enantiomeric pair of Cu_4I_4 cubane-based 1D chain-like hybrid copper(I) iodides, *R*/*S*-**1**, demonstrating ultrabright yellow emissions with chiroptical properties, such as CD and CPL. These materials exhibit both high PLQY to near unity and long-term stability, originating from the rigid structure that suppresses the nonradiative decay. The direct coordination of the chiral ligands and Cu_4I_4 cubane successfully transfer the chiral properties to the inorganic parts, leading to effective CPL emissions. To the best of our knowledge, it is reported here for the first time that CPL-active hybrid copper(I) iodides with near-unity PLQY. Our work on highly emissive and stable hybrid copper(I) iodides paves the way toward the design and construction of high-performance CPL materials.

4. Experimental Section

Materials and General Considerations: All the reagents and solvents, including copper(I) iodide (99%, Macklin), potassium Iodide (99%, Aladdin), ethanol (99%, Rhawn), (*R*)-3-quinuclidinol (98%, Macklin), and (*S*)-3-quinuclidinol (97%, Macklin), were purchased from commercial sources and used without any further purification or modification.

Materials Synthesis: The single crystal samples of Cu_4I_4(*R*/*S*/*Rac*-3-quinuclidinol)$_3$ were prepared by a slow diffusion in a narrow-diameter glass tube (Φ = 15 mm). A saturated KI aqueous solution (2 mL) containing Cu(I)I (0.5 mmol, 95.2 mg) was placed in bottom layer of tube (bottom layer), then a mixture of ethanol (0.5 mL) and water (0.5 mL) was carefully placed on the bottom layer (buffer layer), finally an ethanol (2 mL) of *R*/*S*/*Rac*-3-quinuclidinol (0.5 mmol, 63.6 mg) was placed on the top (top layer). After standing for 1 week, the colorless, plate-like crystals were collected from mother liquid, followed by washing with a large amount of water.

X-Ray Crystallographic Analysis: Single-crystal X-ray diffraction data for all the compounds were recorded on a Bruker D8 VENTURE diffractometer with graphite monochromated Mo Kα radiation (λ = 0.71073 Å). A single crystal was mounted on a thin Kapton film using Nujol and kept at 298 K. The data collection and reduction were carried out using the Bruker APEX3 program for all compounds. The structures were solved by SHELXT methods with the Olex2 program,[65,66] and all non-hydrogen atoms were refined anisotropically by least-squares technique on weighted F^2 using SHELXL.[67] Anisotropic thermal parameters were assigned to all non-hydrogen atoms. The hydrogen atoms attached to C and N atoms were placed in idealized positions. CCDC 2222115 and 2222116 contain the supplementary crystallographic data for Cu_4I_4(*R*-3-quinuclidinol)$_3$ and Cu_4I_4(*S*-3-quinuclidinol)$_3$, respectively. These data can be obtained free of charge from The Cambridge Crystallographic Data Centre (CCDC) via www.ccdc.cam.ac.uk/data_request/cif. Structural diagrams were prepared using VESTA software. Powder X-ray diffraction patterns were collected at room temperature for polycrystalline samples in 0.02° steps on a SmartLab X-ray Diffractometer with Cu Kα radiation (λ = 1.54056 Å).

Optical Characterizations: The steady-state PL spectra were acquired at room temperature using a HORIBA FluoroMax+ instrument (HORIBA Scientific) under an excitation wavelength (λ_{ex}) of 375 nm. The UV–Vis–NIR absorbance spectra were recorded at room temperature on a UV-3600i Plus spectrophotometer (SHIMADZU) with $BaSO_4$ as the reference material. CD spectra for polycrystalline samples were acquired using a CD spectrometer (Chirascan, Applied Photophysics) at room temperature. Polycrystalline samples were carefully packed in the sample chamber without gaps. The measurement was started from 450 to 300 nm with a step of 1 nm. The wavelength and bandwidth of monochromator were 280.0 and 1.0 nm, respectively. Time-per-point of sampling was 0.5 s. PLQYs were examined at room temperature by using the integrating sphere on a XP-EQE-Adv instrument (XI PU GUANG DIAN) (λ_{ex} = 365 nm). For the PL decay measurement, the signal was dispersed by a 320 mm monochromator (iHR320 from Horiba, Ltd.) combined with suitable filters and detected based on the time-correlated single photon counting technique (λ_{ex} = 375 nm). The CPL spectra for powdered samples, which were ground for 15 min, were recorded on a CPL spectrometer (CPL-300, JASCO) (λ_{ex} = 375 nm). The CPL measurement was conducted using a continuous scanning mode with a scanning speed of 2 nm min^{-1}. No. of accumulations was 5.

Supporting Information

Supporting Information is available from the Wiley Online Library or from the author.

Acknowledgements

This work was supported by the National Natural Science Foundation of China (NSFC) under Grant No. 22275077 and the Stable Support Plan Program of Shenzhen Natural Science Fund (Program Contract No. 20220814233319001). The authors are grateful for the assistance of SUSTech Core Research Facilities. J. C. and X. P. contributed equally to this work.

Conflict of Interest

The authors declare no conflict of interest.

Author Contributions

J.C. and X.P. performed the synthesis and characterizations. J.C. drafted the manuscript. L.M. conceived the idea and designed this work. X.Z. conducted the time-resolved PL measurements. All authors have participated in writing the manuscript.

Data Availability Statement

The data that support the findings of this study are available from the corresponding author upon reasonable request.

Keywords

chirality, chiroptics, circularly polarized luminescence, hybrid copper(I) halides, photoluminescence quantum yield

Received: February 2, 2023
Revised: March 1, 2023
Published online: March 18, 2023

[1] Y.-T. Sang, J.-L. Han, T.-H. Zhao, P.-F. Duan, M.-H. Liu, *Adv. Mater.* **2020**, *32*, 1900110.
[2] X.-B. Wang, Y. Wang, W.-Y. Gao, L. Song, C.-X. Ran, Y.-H. Chen, W. Huang, *Adv. Mater.* **2021**, *33*, 2003615.
[3] Z.-G. Wu, H.-B. Han, Z.-P. Yan, X.-F. Luo, Y. Wang, Y.-X. Zheng, J.-L. Zuo, Y. Pan, *Adv. Mater.* **2019**, *31*, 1900524.
[4] F. Zinna, M. Pasini, F. Galeotti, C. Botta, L. Di Bari, U. Giovanella, *Adv. Funct. Mater.* **2017**, *27*, 1603719.
[5] H. K. Bisoyi, Q. Li, *Acc. Chem. Res.* **2014**, *47*, 3184.
[6] F. Zinna, U. Giovanella, L. Di Bari, *Adv. Mater.* **2015**, *27*, 1791.
[7] Y. Yang, R. C. da Costa, M. J. Fuchter, A. J. Campbell, *Nat. Photonics* **2013**, *7*, 634.
[8] C. Wagenknecht, C.-M. Li, A. Reingruber, X.-H. Bao, A. Goebel, Y.-A. Chen, Q. Zhang, K. Chen, J.-W. Pan, *Nat. Photonics* **2018**, *4*, 549.
[9] J.-Y. Wang, C. Zhang, H.-L. Liu, R. McLaughlin, Y.-X. Zhai, S. R. Vardeny, X.-J. Liu, S. McGill, D. Semenov, H.-W. Guo, R. Tsuchikawa, V. V. Deshpande, D.-L. Sun, V. Vardeny, *Nat. Commun.* **2019**, *10*, 129.
[10] Y.-H. Kim, Y.-X. Zhai, H.-P. Lu, X. Pan, C.-X. Xiao, E. A. Gaulding, S. P. Harvey, J. J. Berry, Z. V. Vardeny, J. M. Luther, M. C. Beard, *Science* **2021**, *371*, 1129.
[11] M. C. Heffern, L. M. Matosziuk, T. J. Meade, *Chem. Rev.* **2014**, *114*, 4496.
[12] G. Muller, *Dalton Trans.* **2009**, 9692.
[13] S. C. J. Meskers, *ChemPhotoChem* **2022**, *6*, 20210015.
[14] T.-H. Zhao, J.-L. Han, P.-F. Duan, M.-H. Liu, *Acc. Chem. Res.* **2020**, *53*, 1279.
[15] T. Zhang, K. Xu, J. Li, L. He, D.-W. Fu, Q. Ye, R.-G. Xiong, *Natl. Sci. Rev.* **2022**, *10*, nwac240.
[16] G.-K. Long, R. Sabatini, M. I. Saidaminov, G. Lakhwani, A. Rasmita, X.-G. Liu, E. H. Sargent, W.-B. Gao, *Nat. Rev. Mater.* **2020**, *5*, 423.
[17] Y.-H. Shi, P.-F. Duan, S.-W. Huo, Y.-G. Li, M.-H. Liu, *Adv. Mater.* **2018**, *30*, 1705011.
[18] H.-L. Xuan, J.-L. Li, L.-J. Xu, D.-S. Zheng, Z.-N. Chen, *Adv. Opt. Mater.* **2022**, *10*, 2200591.
[19] J. Chen, S. Zhang, X. Pan, R.-Q. Li, S. Ye, A. K. Cheetham, L.-L. Mao, *Angew. Chem., Int. Ed.* **2022**, *61*, e202205906.
[20] Y. Wei, C. Li, Y.-W. Li, Z.-S. Luo, X.-L. Liu, L.-M. Zhang, X. He, W. Wang, Z.-W. Quan, *Angew. Chem., Int. Ed.* **2022**, *61*, e202212685.
[21] J. Wang, C. Fang, J.-Q. Ma, S. Wang, L. Jin, W.-C. Li, D.-H. Li, *ACS Nano* **2019**, *13*, 9473.
[22] J.-Q. Ma, C. Fang, C. Chen, L. Jin, J.-Q. Wang, S. Wang, J. Tang, D.-H. Li, *ACS Nano* **2019**, *13*, 3659.
[23] C. Han, A. J. Bradford, A. M. Z. Slawin, B. E. Bode, E. Fusco, S. L. Lee, C. C. Tang, P. Lightfoot, *Inorg. Chem.* **2021**, *60*, 11014.
[24] C. Han, A. J. Bradford, J. A. McNulty, W.-G. Zhang, P. S. Halasyamani, A. M. Z. Slawin, F. D. Morrison, S. L. Lee, P. Lightfoot, *Chem. Mater.* **2022**, *34*, 2458.
[25] C. Han, J. A. McNulty, A. J. Bradford, A. M. Z. Slawin, F. D. Morrison, S. L. Lee, P. Lightfoot, *Inorg. Chem.* **2022**, *61*, 3230.
[26] P. C. Ford, E. Cariati, J. Bourassa, *Chem. Rev.* **1999**, *99*, 3625.
[27] X. Zhang, W. Liu, G. Z. Wei, D. Banerjee, Z.-C. Hu, J. Li, *J. Am. Chem. Soc.* **2014**, *136*, 14230.
[28] W. Liu, Y. Fang, J. Li, *Adv. Funct. Mater.* **2018**, *28*, 1705593.
[29] J. Troyano, F. Zamora, S. Delgado, *Chem. Soc. Rev.* **2021**, *50*, 4606.
[30] S.-X. Wang, E. E. Morgan, S. Panuganti, L.-L. Mao, P. Vishnoi, G. Wu, Q.-L. Liu, M. G. Kanatzidis, R. D. Schaller, R. Seshadri, *Chem. Mater.* **2022**, *34*, 3206.
[31] L.-L. Mao, J. Chen, P. Vishnoi, A. K. Cheetham, *Acc. Mater. Res.* **2022**, *3*, 439.
[32] W. Liu, Y. Fang, G. Z. Wei, S. J. Teat, K.-C. Xiong, Z.-C. Hu, W. P. Lustig, J. Li, *J. Am. Chem. Soc.* **2015**, *137*, 9400.
[33] W. Liu, K. Zhu, S. J. Teat, G. Dey, Z.-Q. Shen, L. Wang, D. M. O'Carroll, J. Li, *J. Am. Chem. Soc.* **2017**, *139*, 9281.
[34] L. Yao, G.-D. Niu, J.-Z. Li, L. Gao, X.-F. Luo, B. Xia, Y.-H. Liu, P.-P. Du, D.-H. Li, C. Chen, Y.-X. Zheng, Z.-W. Xiao, J. Tang, *J. Phys. Chem. Lett.* **2020**, *11*, 1255.
[35] J.-J. Wang, H.-T. Zhou, J.-N. Yang, L.-Z. Feng, J.-S. Yao, K.-H. Song, M.-M. Zhou, S. Jin, G.-Z. Zhang, H.-B. Yao, *J. Am. Chem. Soc.* **2021**, *143*, 10860.
[36] X.-Q. Ji, S.-N. Geng, S. Zhang, Y.-P. Gong, X.-Y. Zhang, R.-Q. Li, Y. Liu, J. Chen, R. Chen, Z.-W. Xiao, L.-L. Mao, *Chem. Mater.* **2022**, *34*, 8262.
[37] F. Ge, B.-H. Li, P.-X. Cheng, G. Li, Z.-F. Ren, J.-L. Xu, X.-H. Bu, *Angew. Chem., Int. Ed.* **2022**, *61*, e2021150.
[38] H. Kitagawa, Y. Ozawa, K. Toriumi, *Chem. Commun.* **2010**, *46*, 6302.
[39] S. Perruchas, X. F. Le Goff, S. Maron, I. Maurin, F. Guillen, A. Garcia, T. Gacoin, J.-P. Boilot, *J. Am. Chem. Soc.* **2010**, *132*, 10967.
[40] X.-C. Shan, F.-L. Jiang, L. Chen, M.-Y. Wu, J. Pan, X.-Y. Wan, M.-C. Hong, *J. Mater. Chem. C* **2013**, *1*, 4339.
[41] F. Wei, X.-C. Liu, Z.-W. Liu, Z.-Q. Bian, Y.-L. Zhao, C.-H. Huang, *CrystEngComm* **2014**, *16*, 5338.
[42] S. Yuan, S.-S. Liu, D. Sun, *CrystEngComm* **2014**, *16*, 1927.
[43] Q. Benito, X. F. Le Goff, G. Nocton, A. Fargues, A. Garcia, A. Berhault, S. Kahlal, J.-Y. Saillard, C. Martineau, J. Trébosc, T. Gacoin, J.-P. Boilot, S. Perruchas, *Inorg. Chem.* **2015**, *54*, 4483.
[44] K. Xu, B.-L. Chen, R. Zhang, L. Liu, X.-X. Zhong, L. Wang, F.-Y. Li, G.-H. Li, K. A. Alamry, F.-B. Li, W.-Y. Wong, H.-M. Qin, *Dalton Trans.* **2020**, *49*, 5859.
[45] M. Pronold, M. Scheer, J. Wachter, M. Zabel, *Inorg. Chem.* **2007**, *46*, 1396.
[46] H. El Moll, M. Cordier, G. Nocton, F. Massuyeau, C. Latouche, C. Martineau-Corcos, S. Perruchas, *Inorg. Chem.* **2018**, *57*, 11961.
[47] E. Cariati, E. Lucenti, C. Botta, U. Giovanella, D. Marinotto, S. Righetto, *Coord. Chem. Rev.* **2016**, *306*, 566.
[48] X.-C. Shan, H.-B. Zhang, L. Chen, M.-Y. Wu, F.-L. Jiang, M.-C. Hong, *Cryst. Growth Des.* **2013**, *13*, 1377.
[49] J. P. Safko, J. E. Kuperstock, S. M. McCullough, A. M. Noviello, X.-B. Li, J. P. Killarney, C. Murphy, H. H. Patterson, C. A. Bayse, R. D. Pike, *Dalton Trans.* **2012**, *41*, 11663.
[50] Y. Fang, W. Liu, S. J. Teat, G. Dey, Z.-Q. Shen, L.-T. An, D.-C. Yu, L. Wang, D. M. O'Carroll, J. Li, *Adv. Funct. Mater.* **2017**, *27*, 1603444.
[51] B. Huitorel, H. El Moll, R. Utrera-Melero, M. Cordier, A. Fargues, A. Garcia, F. Massuyeau, C. Martineau-Corcos, F. Fayon, A. Rakhmatullin, S. Kahlal, J.-Y. Saillard, T. Gacoin, S. Perruchas, *Inorg. Chem.* **2018**, *57*, 4328.
[52] B. Huitorel, R. Utrera-Melero, F. Massuyeau, J.-Y. Mevelec, B. Baptiste, A. Polian, T. Gacoin, C. Martineau-Corcos, S. Perruchas, *Dalton Trans.* **2019**, *48*, 7899.
[53] Q.-S. Hu, C.-K. Zhang, X. Wu, G.-J. Liang, L. Wang, X.-W. Niu, Z. Wang, W.-D. Si, Y.-B. Han, R.-Q. Huang, J.-W. Xiao, D. Sun, *Angew. Chem., Int. Ed.* **2023**, *62*, e202217784.
[54] A. Bondi, *J. Phys. Chem.* **1964**, *68*, 441.

[55] H.-X. Miao, X.-C. Pan, M. Li, W.-J. Zhaxi, J. Wu, Z.-T. Huang, L.-Y. Liu, X. Ma, S.-L. Jiang, W. Huang, Q. Zhang, D.-Y. Wu, *Inorg. Chem.* **2022**, *61*, 18779.
[56] P. P. Mazzeo, L. Maini, A. Petrolati, V. Fattori, K. Shankland, D. Braga, *Dalton Trans.* **2014**, *43*, 9448.
[57] L. Yan, M. K. Jana, P. C. Sercel, D. B. Mitzi, W. You, *J. Am. Chem. Soc.* **2021**, *143*, 18114.
[58] H. Ren, Y. Wu, C.-C. Wang, Y. Yan, *J. Phys. Chem. Lett.* **2021**, *12*, 2676.
[59] P. C. Ford, A. Vogler, *Acc. Chem. Res.* **1993**, *26*, 220.
[60] M.-H. Bi, G.-H. Li, J. Hua, X.-M. Liu, Y.-W. Hu, Z. Shi, S.-H. Feng, *CrystEngComm* **2007**, *9*, 984.
[61] K.-H. Song, J.-J. Wang, L.-Z. Feng, F.-X. He, Y.-C. Yin, J.-N. Yang, Y.-H. Song, Q. Zhang, X.-C. Ru, Y.-F. Lan, G.-Z. Zhang, H.-B. Yao, *Angew. Chem., Int. Ed.* **2022**, *61*, e202208960.
[62] M. Hu, F.-Y. Ye, C. Du, W.-Z. Wang, T.-T. Zhou, M.-L. Gao, M.-H. Liu, Y.-S. Zheng, *ACS Nano* **2021**, *15*, 16673.
[63] H. Tsumatori, T. Harada, J. Yuasa, Y. Hasegawa, T. Kawai, *Appl. Phys. Express* **2011**, *4*, 011601.
[64] J. I. Bruce, D. Parker, S. Lopinski, R. D. Peacock, *Chirality* **2002**, *14*, 562.
[65] O. V. Dolomanov, L. J. Bourhis, R. J. Gildea, J. A. K. Howard, H. Puschmann, *J. Appl. Crystallogr.* **2009**, *42*, 339.
[66] G. M. Scheldrick, *Acta Crystallogr.* **2015**, *A71*, 3.
[67] G. M. Sheldrick, *Acta Crystallogr.* **2015**, *71*, 3.